EXTENDED EXPERIMENTAL PROCEDURES

Protein Expression and Purification

The gene encoding mouse cGAS was purchased from Open Biosystems Inc. The sequences corresponding to full-length and residues 147-507 of cGAS were inserted into a modified pRSFDuet-1 vector (Novagen), in which cGAS was separated from the preceding His_6-SUMO tag by an ubiquitin-like protease (ULP1) cleavage site. The gene sequences were subsequently confirmed by sequencing. The fusion proteins were expressed in BL21 (DE3) RIL cell strain. The cells were grown at 37°C until OD600 reached approx. 0.6. The temperature was then shifted to 18°C and the cells were induced by addition of isopropyl β-D-1-thiogalactopyranoside (IPTG) to the culture medium at a final concentration of 0.3 mM. After induction, the cells were grown overnight. The fusion protein was purified over a Ni-NTA affinity column. The His_6-SUMO tag was removed by ULP1 cleavage during dialysis against buffer containing 40 mM Tris-HCl, 0.3 M NaCl, 1 mM DTT, pH 7.5. After dialysis, the protein sample was further fractionated over a Heparin column, followed by gel filtration on a 16/60 G200 Superdex column. The final sample of cGAS (full-length) and cGAS (147-507) contain about 30mg/ml protein, 20 mM Tris, 300 mM NaCl, 1 mM DTT, pH 7.5. The Se-methionine substituted protein was expressed in Se-methionine (Sigma) containing M9 medium and purified using the same protocol used for the wild-type protein. All the mutants were cloned and purified using the same protocol as used for preparation of the wild-type protein.

Crystallization

For crystallization of cGAS (147-507) in the free state, the protein was first diluted into about 15 mg/ml and then mixed with equal volume reservoir solution (0.1 M HEPES, 0.1 M $MgAc_2$, 20% PEG3350, pH 7.6) at 4°C by using hanging drop vapor diffusion method.

For cGAS (147-507)-dsDNA binary complex, the sample was prepared by direct mixing protein with a 16-bp DNA (1-nt 5′-overhang at either end: upper strand 5′- AAATTGCCGAAGACGAA-3′; lower strand 5′- TTTCGTCTTCGGCAATT-3′) in a 1:1.2 molar ratio. The crystals were generated by hanging drop vapor diffusion method at 20°C, from drops mixed from 1 μl of cGAS-dsDNA solution and 1 μl of reservoir solution (0.1 M MES, 8% MPD, pH 6.6). The crystals of Se-methionine substituted cGAS (147-507) in complex with dsDNA were grown under the same condition.

The cGAS (147-507)-dsDNA-ATP, cGAS (147-507)-dsDNA-GTP, and cGAS (147-507)-dsDNA-3′-dGTP ternary complexes were prepared by mixing protein with dsDNA in a 1:1.2 molar ratio, and then incubated in the presence of ATP/GTP/3′-dGTP (5 mM) and $MgCl_2$ (10 mM) for 0.5 hr at room temperature. The crystals for cGAS (147-507)-dsDNA-ATP complex were generated by hanging drop vapor diffusion method at 20°C, from drops mixed from 1 μl of cGAS-dsDNA-ATP solution and 1 μl of reservoir solution (0.1 M HEPES, 0.2 M $CaAc_2$, 20% PEG300, pH 7.7). For cGAS (147-507)-dsDNA-GTP and cGAS (147-507)-dsDNA-3′-dGTP complexes, the crystals were generated by sitting drop vapor diffusion method at 20°C, by mixing equal volume reservoir solution (for GTP: 0.1 M NaAc, 10% MPD, pH 5.0; for 3′-dGTP: 0.1 M NaAc, 12% MPD, pH 5.2) with the samples.

The cGAS (147-507)-dsDNA-GMP+ATP and cGAS (147-507)-dsDNA-GTP+ATP ternary complexes were prepared by mixing protein with dsDNA in a 1:1.2 molar ratio, and then incubated with GMP/GTP (5 mM), ATP (5 mM) and $MgCl_2$ (10 mM) for 0.5 hr at room temperature. The crystals for cGAS (147-507)-dsDNA-GMP+ATP complex were generated by sitting drop vapor diffusion method at 20°C, from drops mixed cGAS-dsDNA-GMP+ATP solution with equal volume reservoir solution (0.1 M MES, 40% MPD, pH 6.0). The crystals for cGAS (147-507)-DNA-GTP+ATP complex were generated over two weeks by sitting drop vapor diffusion method at 20°C, by mixing equal volume reservoir solution (0.1 M HEPES, 0.2 M $MgCl_2$, 30% PEG300, pH 7.5) with the sample.

Structure Determination

The heavy atom derivative crystal of the free state was generated by soaking in a reservoir solution with 5 mM thimerosal for 24h. The diffraction data sets for cGAS (147-507) in free state (both native and Hg-derivative) and DNA-bound state (both native and Se-derivative) were collected at the Brookhaven National Laboratory. The data sets for all the ternary complexes were collected at the Advanced Photo Source (APS) at the Argonne National Laboratory. The diffraction data were indexed, integrated and scaled using the HKL2000 program (Otwinowski and Minor, 1997). The structure of Hg-substituted cGAS (147-507) in free state and Se-substituted cGAS (147-507) in DNA bound state were both solved using single-wavelength anomalous dispersion method as implemented in the program PHENIX (Adams et al., 2010). The model building was carried out using the program COOT (Emsley et al., 2010) and structural refinement was carried out using the program PHENIX (Adams et al., 2010). The statistics of the data collection and refinement for free and binary structures are shown in Table S1. The structures of all the ternary complexes were solved using molecular replacement method in PHASER (McCoy et al., 2007) using the binary structure as the search model. The model building was conducted using the program COOT (Emsley et al., 2010) and structural refinement was conducted using the program PHENIX (Adams et al., 2010). The statistics of the data collection and refinement are shown in Table S2 and S3.

NMR Spectral Analysis of Synthesized cGAMP Linkage Isomers

Lyophilized cGAMP linkage isomers were dissolved in 99.9% D_2O in 10mM K_2HPO_4-KH_2PO_4 (pH 6.6) buffer. All NMR experiments are conducted at 35°C on a Bruker 900 MHz spectrometer at New York Structural Biology Center. Resonance assignments are made based on HMBC (2 s recycling delay, 0.8 s ^1H acquisition time, 20 ms ^{13}C acquisition time, phase-insensitive ^{13}C acquisition, and anti-phase ^1H detection with absolute value mode processing), double-quantum filtered COSY (2 s recycling delay, 0.8 s direct acquisition time, 12 ms indirect acquisition time), and HSQC experiments (1 s recycling delay, 48 ms ^1H acquisition time,

20 ms ^{13}C acquisition time). The 1D proton spectra with water presaturation are accumulated over 8 scans for the synthesized cGAMP linkage isomers standards and 128 scans for the bio-enzymatically produced cGAS reaction.

Preparation of Oligonucleotides for TLC Assays

Oligonucleotides used for biochemical assays of cGAS nucleotidyltransferase activity are listed in Table S6. Oligodeoxynucleotides were synthesized in-house using a 3400 DNA synthesizer (Applied Biosystems), oligoribonucleotides were purchased (Dharmacon). Double-stranded DNA, RNA, and DNA/RNA duplexes were annealed in 70 mM Tris-HCl pH 7.6, 10 mM $MgCl_2$, 5 mM DTT, at equimolar concentrations by incubation initiated at 95°C followed by a 0.1°C decrease per second to 25°C in a Peltier thermocycler (MJ Research), and verified for annealing by agarose gel electrophoresis prior to use.

Thin-Layer Chromatography Analysis of c[G(2′,5′)pA(3′,5′)p] Formation

Purified recombinant full length (fl, amino acids 1-507) and truncated (tr, amino acids 147-507) murine cGAS, including truncated mutant versions 1-6, were incubated in 20 μl reactions containing: 1 μM cGAS, 3.3 μM dsDNA, 5 mM $MgCl_2$, 150 mM NaCl, 20 mM Tris-HCl, pH 7.5 at 25°C, 1 mM DTT, 10% glycerol, 1 mM each of nucleotides (typically ATP and GTP), and $\alpha^{32}P$ or $\gamma^{32}P$ radiolabeled NTPs or dNTPs at 37°C for 40 min. Reactions were stopped by addition of 20 μl of 50 mM EDTA. 2 μl of reaction solution was spotted onto high-performance TLC plates (HPTLC silica gel, 60 Å pores, F_{254}, 10x10 cm, cat # 1.05628.0001, EMD Millipore) and products were separated with Solvent 1 (NH_4HCO_3:C_2H_5OH:H_2O [0.2 M:30%:70%], w:v:v) or 2 (NH_4HCO_3:C_2H_5OH:H_2O [0.025 M:30%:70%], w:v:v) at 25°C for 1 hr. Reaction products were visualized by UV (254 nm) and phosphorimaging (Typhoon FLA 9500, GE Healthcare). Images were processed using Adobe Photoshop and Illustrator CS5. The TLC conditions used were largely based on a protocol established to separate 3′,5′ cAMP (Higashida et al., 2002).

Quantitation of cGAS Reaction Products

The yield of c[G(2′,5′)pA(3′,5′)p] generated was calculated by densitometry analysis of TLC experiments, using FIJI (ImageJ 1.47i) or spectrophotemetrically (absorbance at 260 nm, $E_{260} = 25.4 \times 10^3$) after purification from HPLC. For densitometry analyses, the fraction of $\alpha^{32}P$-labeled c[G(2′,5′)pA(3′,5′)p] over total radioactivity per lane (c[G(2′,5′)pA(3′,5′)p] plus remaining $\alpha^{32}P$-labeled ATP or GTP) was calculated.

Preparation of cGAS Reaction Products for High-Performance Liquid Chromatography Analysis

In vitro generated c[G(2′,5′)pA(3′,5′)p] reaction products, or washed and dissolved cGAS crystals, were treated with 25 units of Benzonase (Novagen, cat. # 70746, Purity > 90%) for 30 min at 37°C, heat inactivated for 10 min at 95°C, then centrifuged at 21,000 g for 15 min (Sorvall Legend Micro 21R, Thermo Scientific); the supernatant was used for HPLC analysis. Reaction products, with or without 3-8 nmoles of chemically synthesized all 3′,5′ cGAMP, all 2′,5′ cGAMP, or c[G(2′,5′)pA(3′,5′)p] were subjected to reverse-phase HPLC analysis (AKTA Purifier, GE Healthcare) using a C18 column (25 cm x 4.5 mm, 5 μM pore, Supelco Analytical). Analytes were monitored by UV 260 and 280 nm. A 0%–10% solvent B (2 column volume), 10%–50% solvent B (2 column volume) two-step linear gradient was used; solvent A (triethylammonium acetate:acetonitrile:H_2O [0.1 M:3%:97%], w:v:v) and solvent B (methanol:acetonitrile:H_2O [45%:45%:10:], v:v:v).

Preparation of cGAS Reaction Product for 1D NMR Analysis

100 μl of in vitro generated c[G(2′,5′)pA(3′,5′)p] reaction product was benzonase and heat treated as before, prior to fractionation by HPLC. Three serial HPLC runs were performed (two 40 μl and one 20 μl reaction injection), and the peak corresponding to c[G(2′,5′)pA(3′,5′)p] was collected into a 15 ml falcon tube (approx. 4.5 ml total). Solvent removal was accomplished by vacuum centrifuge (Vacufuge, Eppendorf) for 3 days at room temperature until completely dry.

Generation of cGAS Point Mutants for Cellular Assays

The murine cGAS CDS was inserted into a modified pMAX-cloning vector (Amaxa, Cologne, Germany). Site-directed mutagenesis was performed using the Quikchange method (Agilent, Santa Clara, CA) using Pfu Ultra Hot Start DNA Polymerase (Agilent) or KOD Hot Start DNA Polymerase (Merck, Darmstadt, Germany). The murine STING CDS and Firefly Luciferase (Promega, Madison, WI) were cloned into an EF1-promoter- modified pLenti6 (Invitrogen, Carlsbad, CA) expression plasmid. pGL3 IFN-beta Gluc reporter was a kind gift from Brian Monks (Institute of Innate Immunity, University of Bonn, Germany). All constructs were verified by sequencing of the CDS.

Luciferase Assay

$3x10^4$ HEK293 cells per 96-well were reverse-transfected in triplicates with a mixture of pGL3-IFNbeta-Gluc (50 ng), pLenti-EF1-Fluc (25 ng), pLenti-EF1-mSTING (25 ng) and cGAS-expression plasmid (25ng, pMAX-cGAS WT or mutants) or Control plasmid pMAX-GFP (Amaxa) using Trans-IT LT1 (MirusBio, Madison, WI). After 36 hr cells were lysed in passive lysis buffer. Firefly and gaussia Luciferase activities were determined on an EnVision reader (Perkin Elmer, Waltham, MA) using the respective substrates D-luciferin and coelenterazine(PJK GmbH, Kleinblittersdorf, Germany). IFNbeta-Gluc values were normalized to constitutive firefly luciferase values and fold induction was calculated in relation to control-plasmid pMAX-GFP.

Synthesis of Cyclic GA Dinucelotides

Preparation of all 2′,5′-cGAMP (6, Figure S7), c[G(2′,5′)pA(3′,5′)p] (11, Figure S7), and all 3′,5′-cGAMP (15, Figure S7) were carried out using the procedure previously reported by the Jones laboratory (Gaffney et al., 2010; Gaffney and Jones 2012). To adenosine phosphoramidite, 1 or 7, (0.784 g, 0.793 mmol) dissolved in 5 ml of CH_3CN and water (0.028 ml, 1.6 mmol, 2 equiv) was added pyridinium trifluoroacetate (0.184 g, 0.95 mmol, 1.2 equiv). After 1 min, 6 ml of *tert*-$BuNH_2$ was added. After another 10 min, the mixture was concentrated. To the residue dissolved in 10 ml of CH_2Cl_2 was added H_2O (0.14 ml, 7.9 mmol, 10 equiv), followed by 10 ml of 6% dichloroacetic acid (DCA, 7.5 mmol) in CH_2Cl_2. After 10 min, the reaction was quenched by addition of pyridine (1.2 ml, 15 mmol, 2 equiv rel to DCA). The mixture was then concentrated, and the residue was dissolved in 7 ml of CH_3CN and concentrated again. This process was repeated two more times, the last time leaving the A H-phosphonate, 2 or 8, in 2 ml. To this solution was added a dried solution of G amidite, 3 or 12 (1.00 g, 1.03 mmol, 1.3 equiv) in 3 ml CH_3CN. After 2 min, anhydrous *tert*-butyl hydroperoxide 5.5 M in decane (0.43 ml, 2.4 mmol, 3 equiv) was added. After 30 min, 0.20 g of $NaHSO_3$ dissolved in 0.5 ml H_2O was added. The mixture was stirred for 5 min, and then concentrated. The residual oil was dissolved in 14 ml of CH_2Cl_2, followed by addition of H_2O (0.15 ml, 8.5 mmol, 10 equiv) and then 14 ml of 6% DCA (9.8 mmol) in CH_2Cl_2. After 10 min, the reaction was quenched with 9 ml of pyridine. The mixture was concentrated to a small volume, 25 ml more pyridine was added, and the solution was concentrated again, leaving the linear dimer, 4, 9, or 13, in 17 ml. To this solution was added 5,5-dimethyl-2-oxo-2-chloro-1,3,2-dioxaphosphinane (DMOCP, 0.54 g of 95% reagent, 2.8 mmol, 3.5 equiv). After 10 min, the reaction was quenched by addition of H_2O (0.50 ml, 28 mmol, 10 equiv rel to DMOCP), and I_2 (0.26 g, 1.0 mmol, 1.3 equiv) was added immediately. After 5 min, the mixture was poured into 120 ml of H_2O containing 0.17 g $NaHSO_3$. After 5 min of stirring, 3.4 g of $NaHCO_3$ was slowly added. After 5 min more of stirring, the aqueous solution containing solid was partitioned with 135 ml 1:1 EtOAc:Et_2O. The separated aqueous layer was then partitioned with an additional 35 ml of 1:1 EtOAc:Et_2O. The organic layers containing 5, 10, or 14 were combined and concentrated to an oil. For 14, the oil was dissolved in 5 ml CH_3CN and the cyanoethyl group was removed by addition of 5 ml of *tert*-$BuNH_2$ for 10 min. The residue was purified on a 80 g SiO_2 column, using a gradient of 0 to 25% CH_3OH in CH_2Cl_2 over 50 min. 5 and 10 were directly purified on SiO_2 without *tert*-$BuNH_2$ treatment. In each case the residue after purification was treated with 21 ml of CH_3NH_2 in anhydrous EtOH (33% by weight, 168 mmol, 212 equiv rel to the amino protecting groups). After 4 hr at room temperature, the mixture was concentrated to a solid, to which 3 ml of pyridine and 1 ml of Et_3N were added. The mixture was concentrated to an oil, and this process was repeated two more times to convert the *tert*-$BuNH_3^+$ to the Et_3NH^+ salt. To the oil was added 1mL of pyridine, and the flask was placed in an oil bath at 55°C. Et_3N (7.5 ml) and $Et_3N{\cdot}3HF$ (2.6 ml, 48 mmol F^-, 30 eq rel to each TBS) were added simultaneously. The mixture was stirred at 55°C. After 3 hr, the flask was removed from the oil bath and HPLC grade acetone (70 ml) was slowly added to the stirring mixture. After 10 min, the solid was collected by filtration, washed 5x with 3 ml portions of acetone, and dried in a desiccator over KOH overnight. This process gave pure 15, but 6 and 11 were purified on a 19x300 mm Prep Nova-Pak C18 column using a gradient of 2 to 20% CH_3CN in 0.1 M NH_4HCO_3.

Analytical reversed phase HPLC was carried out on a Waters 2965 system with a photodiode array detector, using an Atlantis C18 column, 100 Å, 4.6 mm × 50 mm, 3.0 μm. Gradients of CH_3CN and 0.1 M triethylammonium acetate buffer (pH 6.8) were used with a flow rate of 1.0 ml/min. Low resolution ESI-MS was routinely acquired using a Waters Micromass single quadrupole LCZ system. LCMS of 6, 11, and 15 displayed *m/z* (M-H) 673 (calculated for $C_{20}H_{23}N_{10}O_{13}P_2^-$: 673).

SUPPLEMENTAL REFERENCES

Adams, P.D., Afonine, P.V., Bunkóczi, G., Chen, V.B., Davis, I.W., Echols, N., Headd, J.J., Hung, L.W., Kapral, G.J., Grosse-Kunstleve, R.W., et al. (2010). PHENIX: a comprehensive Python-based system for macromolecular structure solution. Acta Crystallogr. D Biol. Crystallogr. *66*, 213–221.

Emsley, P., Lohkamp, B., Scott, W.G., and Cowtan, K. (2010). Features and development of Coot. Acta Crystallogr. D Biol. Crystallogr. *66*, 486–501.

Higashida, H., Hossain, K.Z., Takahagi, H., and Noda, M. (2002). Measurement of adenylyl cyclase by separating cyclic AMP on silica gel thin-layer chromatography. Anal. Biochem. *308*, 106–111.

McCoy, A.J., Grosse-Kunstleve, R.W., Adams, P.D., Winn, M.D., Storoni, L.C., and Read, R.J. (2007). Phaser crystallographic software. J. Appl. Cryst. *40*, 658–674.

Otwinowski, Z., and Minor, W. (1997). Processing of X-ray Diffraction Data Collected in Oscillation Mode. Methods Enzymol. *276*, 307–326.

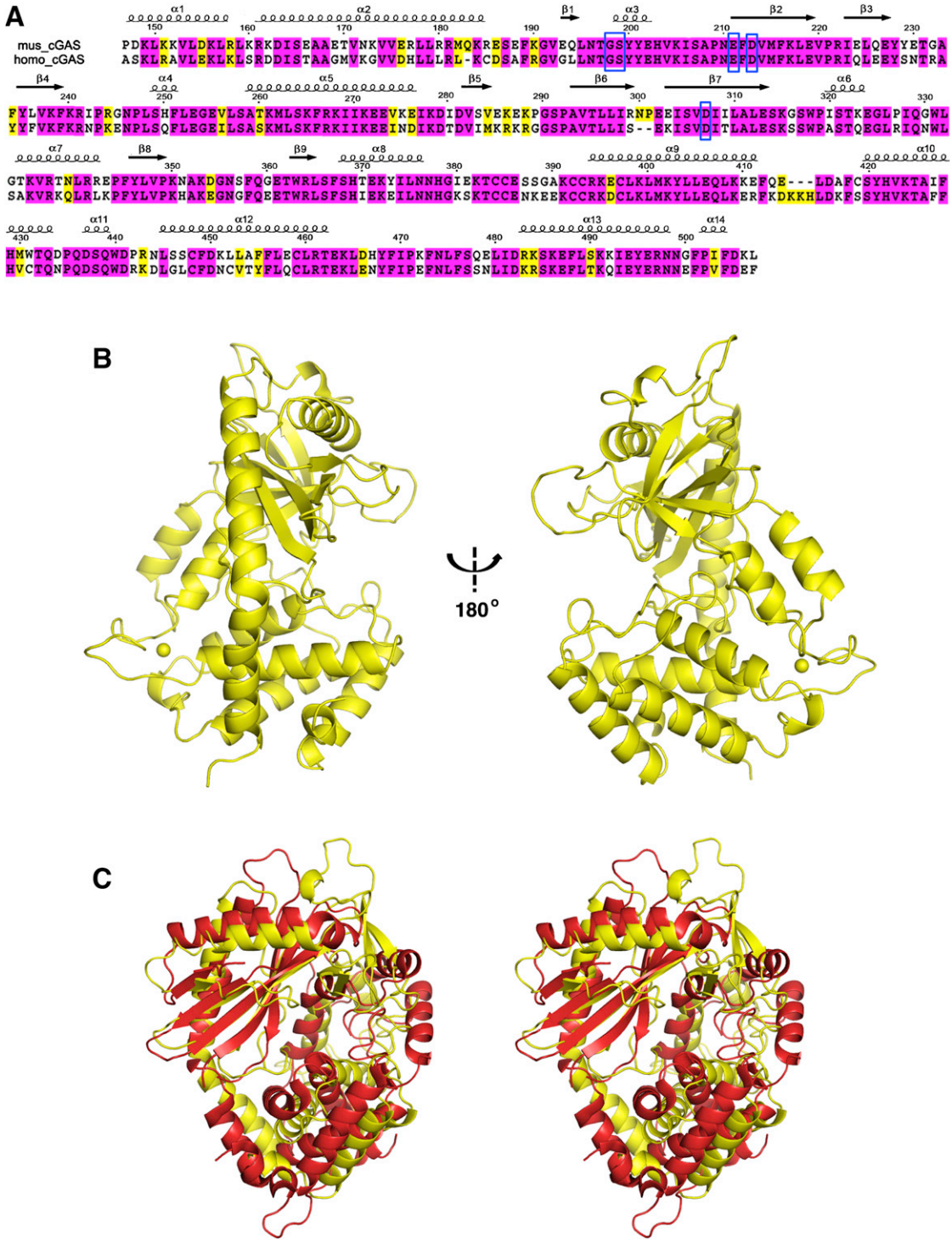

Figure S1. Sequence Alignment and Crystal Structure of cGAS in the Free State and Comparison with Human OAS1, Related to Figure 1

(A) Sequence alignment of cGAS from mouse and human (construct used for structural studies) spanning amino acids 147 to 507 (C terminus). The putative catalytic residues are indicated in blue boxes.

(B) Two alternate views of the structure of cGAS in the free state. The backbone of the protein is shown in a ribbon representation and colored in yellow.

(C) Stereo view of superposed structures of cGAS (yellow) and human oligoadenylate synthetase 1 (OAS1) (red; PDB: 1PX5) in the free state. The rmsd between structures is 4.1 Å.

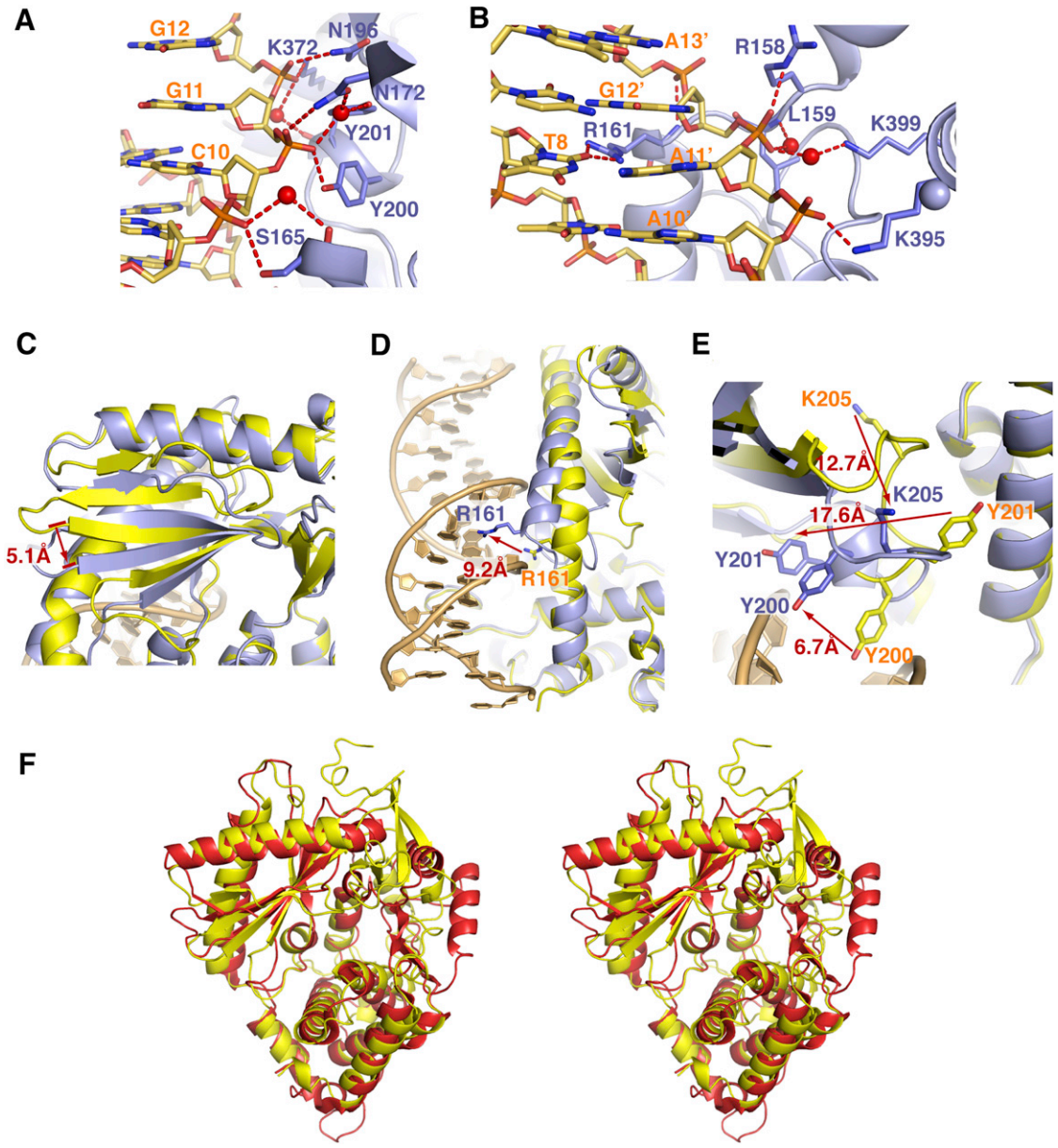

Figure S2. Molecular Recognition Features in the Structure of cGAS Bound to dsDNA and Comparison with hOAS1 Bound to dsRNA and 2′-dATP, Related to Figure 1

(A and B) Examples of intermolecular contacts between cGAS and dsDNA. Water molecules are shown as red spheres, with hydrogen bonds are indicated by dashed red lines. We observe one sequence-specific hydrogen bond between the side chain of Arg161 and the O2 carbonyl of T8 as shown in (B).

(C–E) Examples of conformational shifts on proceeding from cGAS in the free state (yellow) to the binary complex with bound dsDNA (blue). A shift of 5.1 Å is observed in the β sheet segment on complex formation (C). A long α-helix breaks into two segments, with one segment moving toward the dsDNA on complex formation, including the side chain of Arg161, which moves by 9.2 Å (D). Several Tyr and Lys residues within loop segments shift between 6.7 and 17.6 Å on complex formation (E).

(F) Stereo view of the superposed structures of the protein components of cGAS in the dsDNA bound state (yellow) and OAS1 in the dsRNA bound state plus 2′-dATP (red, PDB: 4IG8). The rmsd between structures is 3.2 Å. The dsDNA bound to cGAS and dsRNA bound to OAS1 are omitted from depiction for clarity.

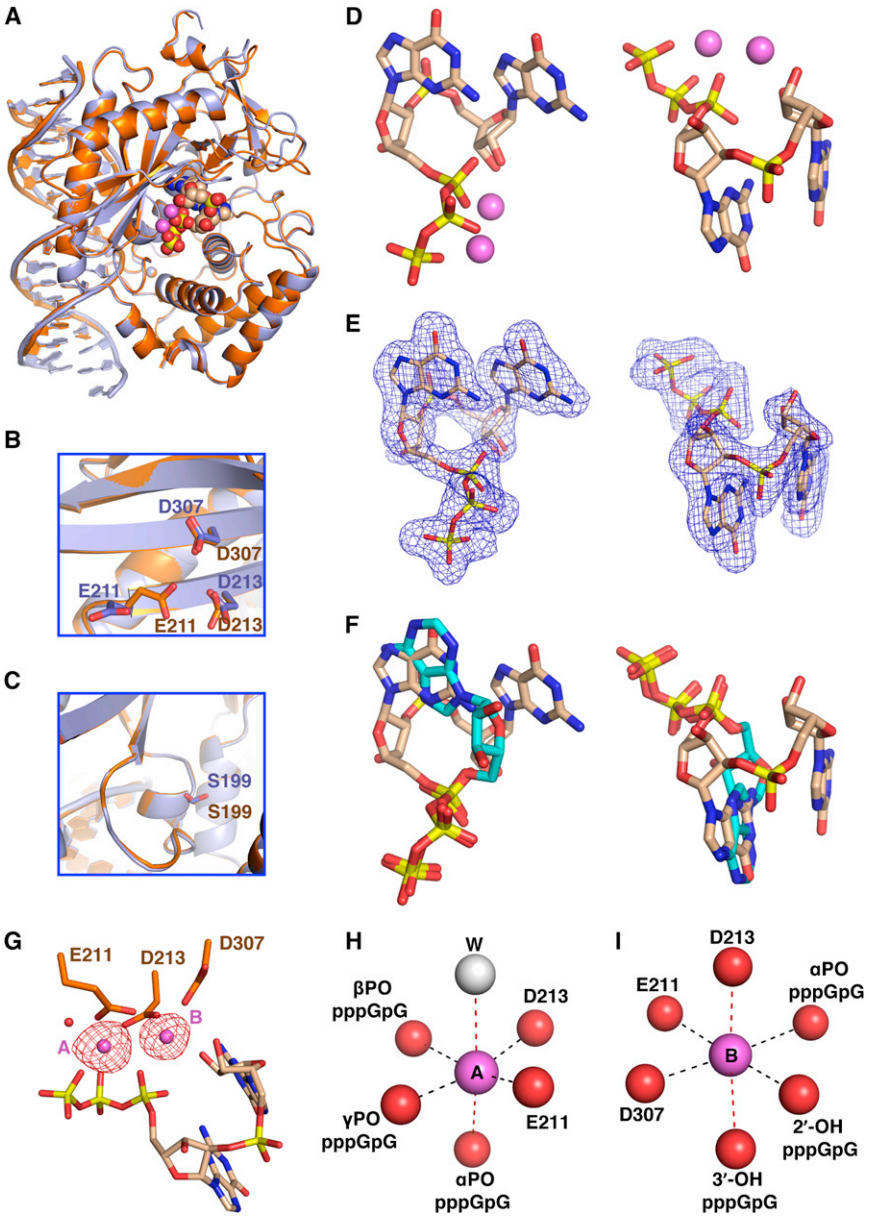

Figure S3. Structure of cGAS with 5′-pppG(2′,5′)pG in the Catalytic Pocket of Its Ternary Complex Formed upon Crystallization with GTP, Related to Figure 3

(A) Superposed structures of the binary complex of cGAS with DNA (blue) and the ternary complex with bound 5′-pppG(2′,5′)pG intermediate product (orange).

(B and C) Minimal changes are observed in the backbone within the β sheet (B) and catalytic pocket (C) segments on proceeding from the binary complex (in blue) to the ternary complex with bound 5′-pppG(2′,5′)pG (to orange).

(D) Two alternate views of the bound 5′-pppG(2′,5′)pG in the catalytic pocket of the ternary complex. Mg^{2+} cations are shown as magenta spheres. Note that the alignment of bound ligand is 5′-pppG(*syn*)p(2′,5′)pG(*anti*).

(E) Two alternate views of the omit Fo-Fc omit electron density map contoured at 3.0σ (blue) of bound 5′-pppG(2′,5′)pG in the catalytic pocket of the ternary complex.

(F) Two alternate views of the superposed structures of bound 5′-pppG(2′,5′)pG (biscuit) and ATP (cyan) in their respective ternary complexes with cGAS and dsDNA.

(G) Omit map recorded at 4σ identifying two bound cations in the structure of the ternary complex.

(H and I) Octahedral coordination geometry around the two bound cations in the structure of the ternary complex.

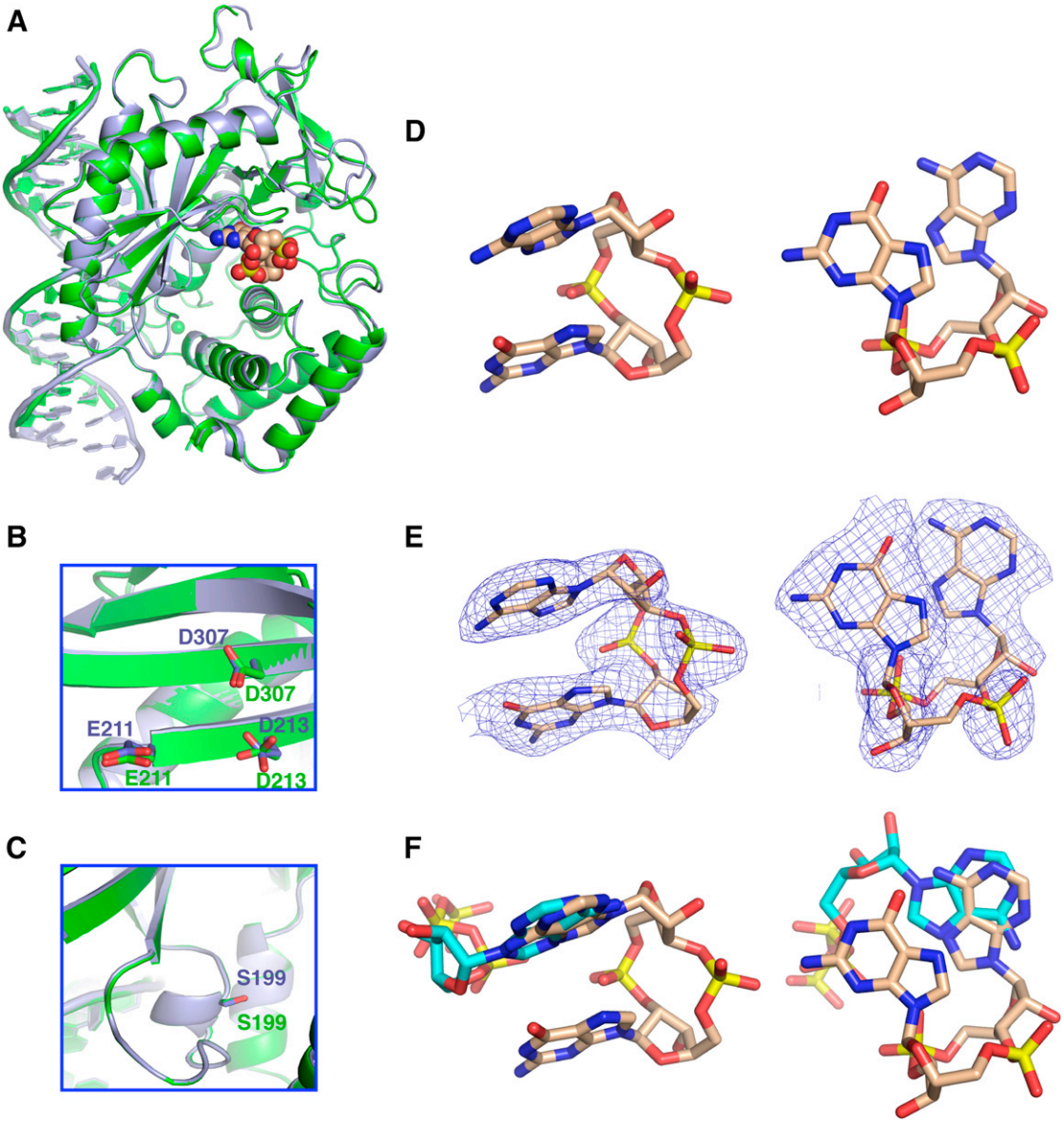

Figure S4. Structure of cGAS and c[G(2′,5′)pA(3′,5′)p] Bound in the Catalytic Pocket of the Ternary Complex Formed upon Crystallization with GTP + ATP, Related to Figure 4

(A) Superposed structures of the binary complex of cGAS and DNA (blue) and the ternary complex with added GTP+ATP for which the bound product is c[G(2′,5′)pA(3′,5′)p] (green) obtained from crystallization with ATP and GTP.

(B and C) No conformational changes occurred in the backbone within the β sheet (B) and catalytic pocket (C) segments on proceeding from the binary complex (in blue) to the ternary complex with bound c[G(2′,5′)pA(3′,5′)p] (in green).

(D) Two alternate views of the bound product cGAMP in the catalytic pocket of the ternary complex. Note that the bound ligand c[G(2′,5′)pA(3′,5′)p] revealed a 2′,5′ phosphodiester linkage within the GpA step. Based on HPLC comparison, the structure of c[G(2′,5′)pA(3′,5′)p] is shown with a 3′,5′ linkage at the ApG step. Both G and A residues adopt *anti* alignments at their glycosidic bonds.

(E) Two alternate views of the Fo-Fc omit electron density map contoured at 3.0σ (blue) of bound c[G(2′,5′)pA(3′,5′)p] in the catalytic pocket of the ternary complex.

(F) Two alternate views of the superposed structures of bound c[G(2′,5′)pA(3′,5′)p] (biscuit) and ATP (cyan) in their respective ternary complexes with cGAS and dsDNA.

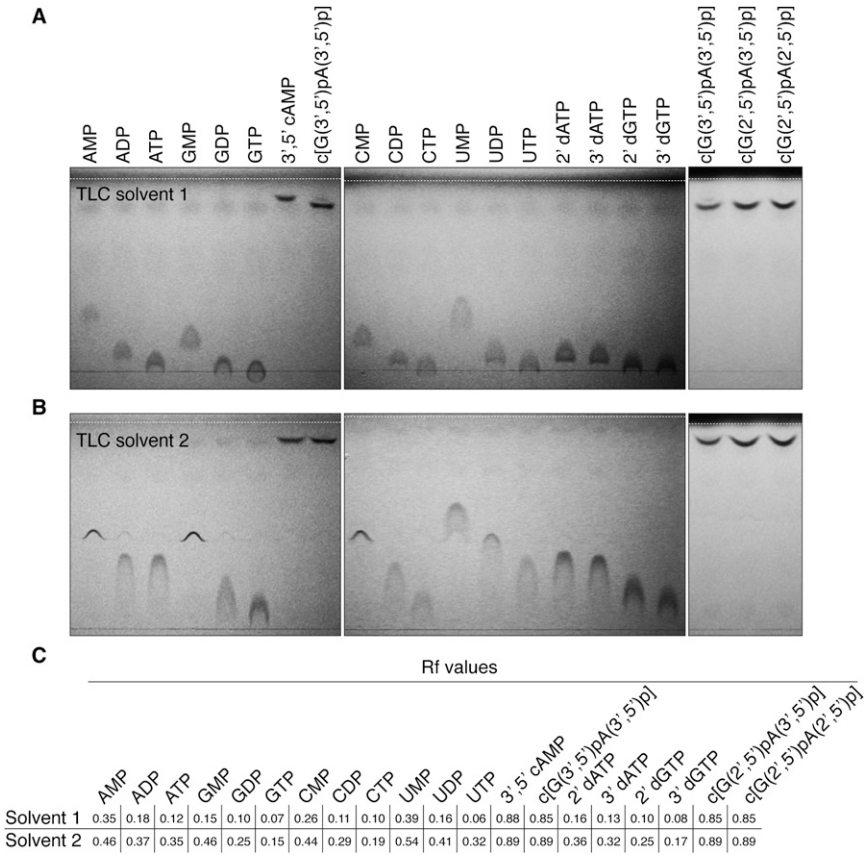

	AMP	ADP	ATP	GMP	GDP	GTP	CMP	CDP	CTP	UMP	UDP	UTP	3',5' cAMP	c[G(3',5')pA(3',5')p]	2' dATP	3' dATP	2' dGTP	3' dGTP	c[G(2',5')pA(3',5')p]	c[G(2',5')pA(2',5')p]
Solvent 1	0.35	0.18	0.12	0.15	0.10	0.07	0.26	0.11	0.10	0.39	0.16	0.06	0.88	0.85	0.16	0.13	0.10	0.08	0.85	0.85
Solvent 2	0.46	0.37	0.35	0.46	0.25	0.15	0.44	0.29	0.19	0.54	0.41	0.32	0.89	0.89	0.36	0.32	0.25	0.17	0.89	0.89

Figure S5. Thin-Layer Chromatography Conditions for Monitoring Formation of cGAMP, Related to Figure 5

(A and B) Indicated nucleotides were spotted on high-performance silica gel thin-layer chromatography (TLC) plates, resolved by various solvent systems, and visualized by UV. Two mobile phase conditions were used (A and B). Solvent system 1 was used in the majority of experiments for detection of c[G(2′,5′)pA(3′,5′)p], whereas solvent 2 was used for a better separation of the mono and tri-phosphorylated linear intermediates. Dashed lines indicate the solvent fronts.

(C) Calculated Rf values.

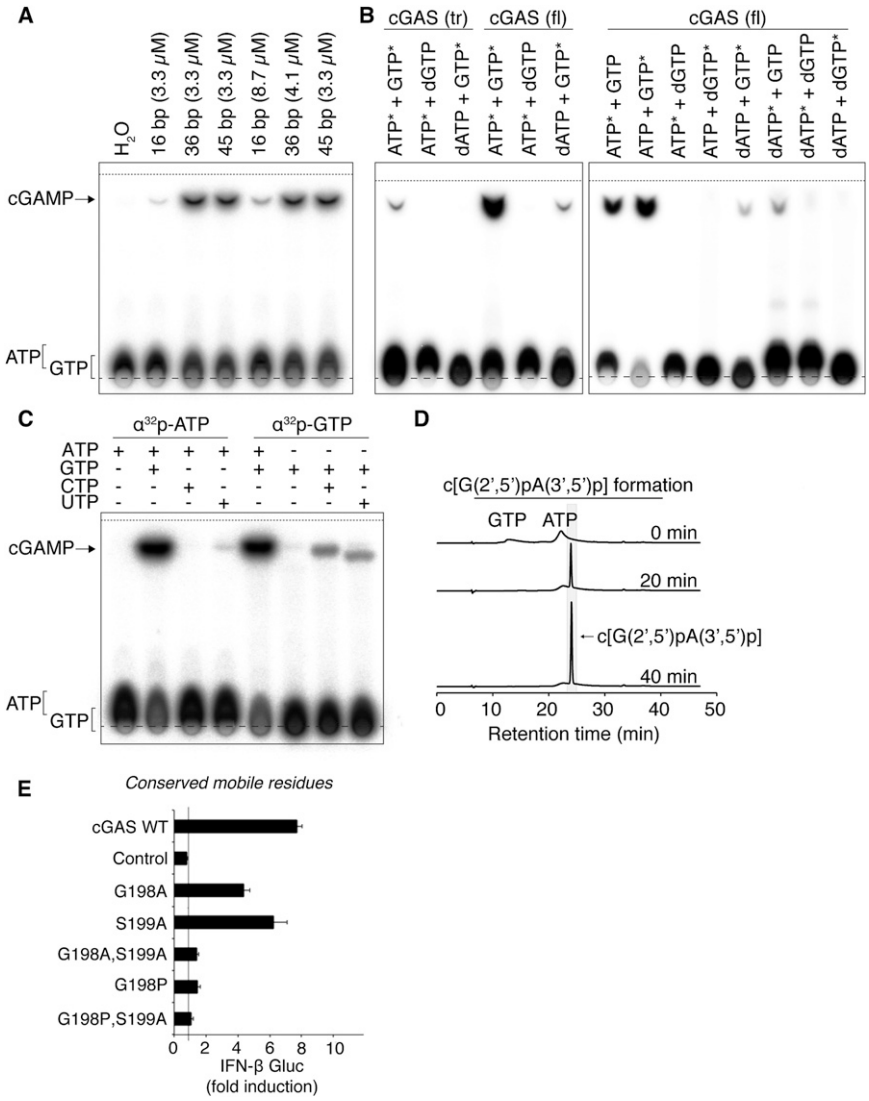

Figure S6. dsDNA Length and Nucleotide Requirements of cGAS Activity, Related to Figures 5 and 7

(A) Full-length cGAS was incubated with equimolar or mass-normalized quantities of 16-, 36-, or 45-nt dsDNA then assayed for cGAMP formation. Long- and short-dashed lines in panels A-C, indicate the origin and solvent fronts, respectively.

(B) Truncated (tr) and full-length (fl) cGAS was incubated with 45 bp dsDNA in reaction buffer containing the various indicated nucleotides. cGAS (tr) exhibits activity, albeit less than cGAS (fl). c[G(2′,5′)pA(3′,5′)p] forms using 2′-dATP, when 2′-dATP or GTP was radiolabelled, but not at all when 2′-dGTP was used. 2′-dATP with 2′-dGTP yielded no c[G(2′,5′)pA(3′,5′)p], indicating that blockage of the 2′ OH positions in adenosine, and more importantly guanosine, prevented c[G(2′,5′)pA(3′,5′)p] production. Asterisks (*) denote which nucleotides were supplemented with an α^{32}p-radiolabelled form. dNTP indicates the triphosphorylated 2′-deoxynucleotide.

(C) Full-length cGAS was incubated in reaction buffer containing dsDNA and the indicated combination of ribonucleotides, then analyzed by TLC. Trace amounts of cyclic product were formed upon incubation of α^{32}p-ATP with UTP, or α^{32}p-GTP with GTP, CTP, and UTP. Optimal product formation requires GTP and ATP. The low level of cyclic product formation with UTP and ATP, but no ATP alone, suggests that UTP can be accommodated at the GTP binding site but reduced in affinity and/or activity. The migrations of all products are consistent with formation of cyclical dinucleotides.

(D) HPLC analysis of dsDNA-dependent cGAS generation of c[G(2′,5′)pA(3′,5′)p] over time. A single cGAS reaction was initiated and samples were analyzed by HPLC at indicated times.

(E) Highly conserved residues G198 and S199 were mutated to alanine, or G198 to proline to reduce steric flexibility. Expression plasmids for mutant and WT cGAS were transiently transfected into HEK293 cells together with an IFN-β Gluc reporter, and constitutive STING and Firefly luc expression plasmids. Gluc values were determined in triplicate, 36 hr after transfection, normalized to Firefly luc, and are shown as fold induction over Control plasmid (as mean ± SEM). Data are representative of 3 independent experiments for each mutant.

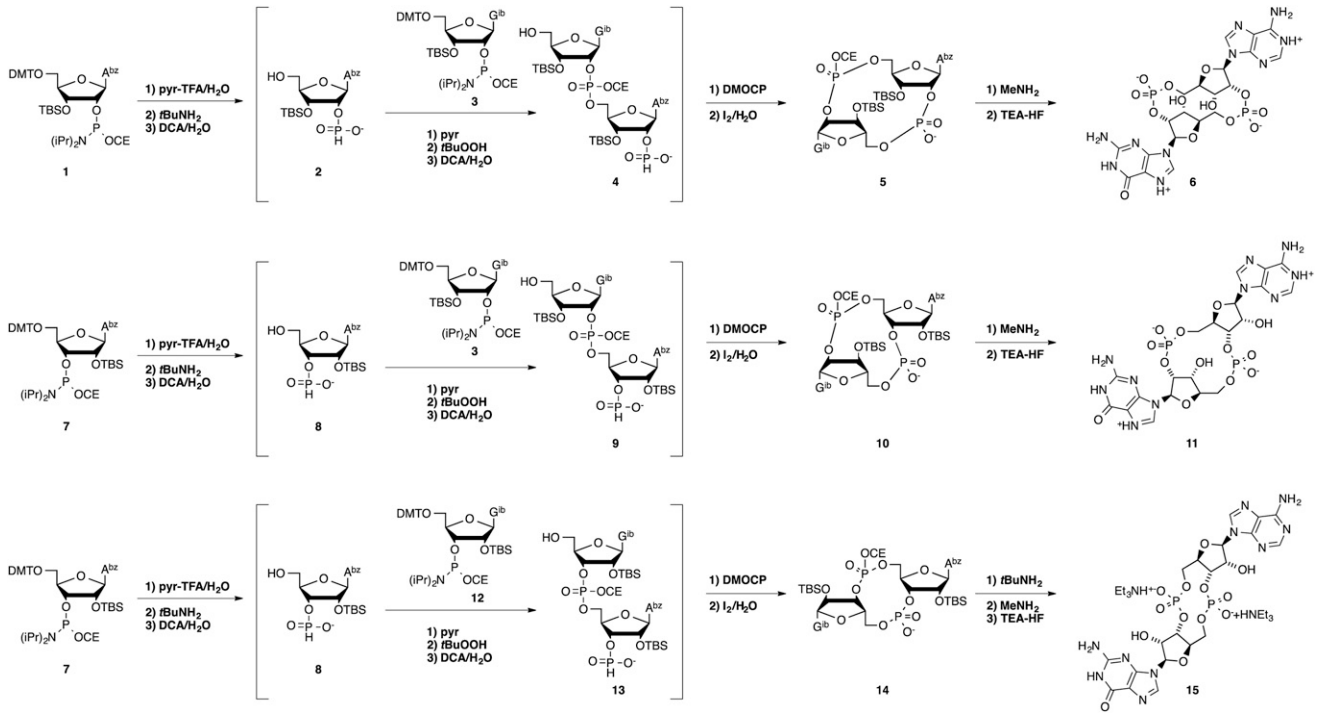

Figure S7. Syntheses of cGAMP Isomers, Related to Figure 6

(Top) Synthesis of cGAMP containing 2′,5′ linkages at both GpA and ApG steps (6). (Middle) Synthesis of cGAMP containing 2′,5′ at GpA step and 3′,5′ at ApG step (11). (Bottom) Synthesis of cGAMP containing 3′,5′ linkages at both GpA and ApG steps (15).

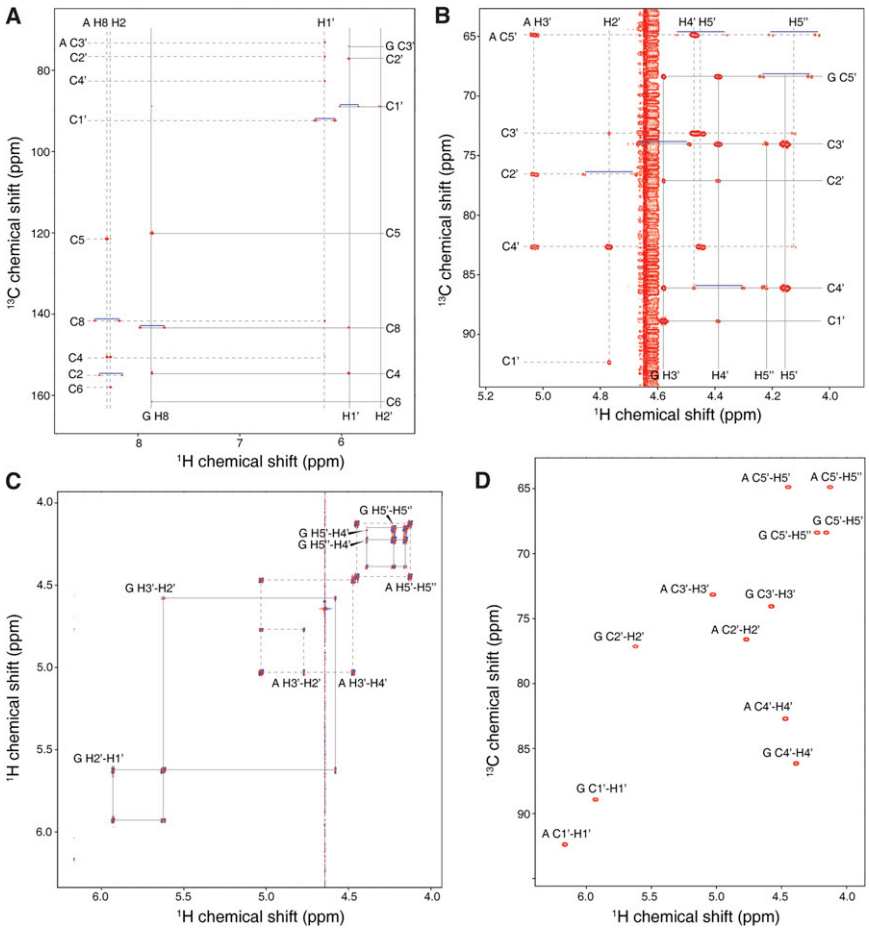

Figure S8. Resonance Assignments of c[G(2′,5′)pA(3′,5′)p] from HMBC, COSY, and HSQC Two-Dimensional NMR Spectra, Related to Figure 6

(A) HMBC spectrum showing correlations between aromatics and the sugar C1'-H1'.

(B) HMBC spectrum showing correlations within sugar rings. In (A) and (B), correlations within the guanine base are connected by solid lines and assignments are specified on the upper and left edges for protons and carbons respectively, while correlations within the adenine base are connected by dashed lines and assignments are specified on the lower and right edges for protons and carbons respectively; The large unsuppressed 1-bond C-H couplings are indicated by blue lines connecting the coupled pairs of signals.

(C) Double quantum filtered COSY spectrum. Guanine correlations are connected by solid lines and resonances are labeled on the cross peaks above the diagonal; Adenine correlations are connected by dashed lines and resonances are labeled on the cross peaks below the diagonal.

(D) Aliphatic HSQC spectrum summarizing sugar proton and carbon assignments.